

# 改性 J422 焊条电弧焊碳钢接头在亚硫酸铵溶液中的耐蚀性

雷阿利, 张盛超, 张 敏

(西安理工大学 材料科学与工程学院, 西安 710048)

**摘 要:** 针对亚硫酸铵介质中碳钢焊接接头腐蚀严重的实际, 采用向普通碳钢焊条 J422 药皮中添加镍的方法, 以三电极电化学研究方法和金相组织分析法研究了焊缝不同含镍量情况下碳钢焊接接头在亚硫酸铵溶液中的腐蚀行为。结果表明, 镍元素的加入使得焊缝组织晶粒细化, 针状铁素体减少; 同时提高了碳钢焊接接头的自腐蚀电位; 焊接接头在亚硫酸铵溶液中的极化率增大, 自腐蚀电流减小; 其中焊缝 Ni 元素含量为 1.2% 的焊接接头腐蚀速率最小。

**关键词:** 亚硫酸铵; 焊缝腐蚀; 合金化; 电化学

**中图分类号:** TG174 **文献标识码:** A **文章编号:** 0253-360X(2007)07-029-04



雷阿利

## 0 序 言

亚硫酸铵法制浆效率高, 强度好, 滤水性强, 废液可直接灌溉农田, 且能更好地利用硫酸铵资源, 因而被许多造纸厂采用。但亚硫酸铵对制浆设备腐蚀严重, 未加保护的蒸球, 轻者腐蚀率为 0.515 mm/a, 严重者达 3.24 mm/a<sup>[1]</sup>, 蒸球焊缝腐蚀引起的爆炸屡屡发生。碳钢焊接接头在亚硫酸铵介质中腐蚀时, 焊缝区电位低于母材显阳极, 母材为阴极, 这便形成了大阴极小阳极的腐蚀体系, 导致碳钢焊接接头成为整个构件中的最薄弱环节。文献[2]研究了 Q235 钢焊接接头在亚硫酸铵介质中的腐蚀行为, 但如何降低碳钢焊接接头在亚硫酸铵介质中的腐蚀速率却未见报道。针对这种情况, 考虑提高焊缝的电位, 使得整个母材为阳极, 焊缝为阴极, 构成大阳极小阴极的腐蚀体系<sup>[3]</sup>。由于镍的电位比铁高, 又具有细化晶粒的作用, 研究向焊缝过渡镍合金元素, 提高焊缝电极混合电位或腐蚀电位<sup>[3-5]</sup>, 从而提高碳钢焊缝在亚硫酸铵介质中的耐蚀性, 为亚硫酸铵法制浆设备的腐蚀与防腐提供参考。

## 1 试 验

### 1.1 试验原料及器材

试验原料为 (NH<sub>4</sub>)<sub>2</sub>SO<sub>3</sub>·H<sub>2</sub>O (化学纯)。

试验器材为 HDV-7C 晶体管恒电位仪、GX-1 给定信号发生器、DK-98-1 电子恒温水浴锅、电子分析天平等。

工作电极采用 Q235 钢焊接接头, 铂电极为辅助电极, 参比电极为饱和甘汞电极 (SCE)。

### 1.2 试验方法

焊条制备, 采用 H08A 焊芯, 在药皮中加入金属镍粉 (粒度 400 目, 纯度 99%), 以焊芯重量为基础, 计算镍的加入量, 药皮采用酸性药皮。

试样制备, 将厚 4 mm 的 Q235 钢板分别用 J422 焊条以及自制改性焊条手工交流电弧焊对焊连接, 电弧电压 30 V, 焊接电流 110 A。然后将得到的不同焊接接头整体按  $S_{\text{焊缝}}:S_{\text{母材}}=1:1$  取下。分别记为 1 号、2 号、3 号、4 号、5 号, 其中 1 号为采用 J422 焊条焊接的接头, 2 号、3 号、4 号分别为焊缝 Ni 元素含量为 0.8%, 1.2%, 1.5% 的焊接接头, 5 号为母材。再将制备好的试样分别用导线连接, 用环氧树脂封装非研究面制成研究电极。测试前用金相砂纸逐级打磨至镜面, 用酒精去脂, 去离子水冲洗, 干燥后备用。

极化曲线的测量, 采用三电极电化学腐蚀体系, DK-98-1 电子恒温水浴锅控制温度, 待试样表面在溶液中稳定 15 min 后测试其自腐蚀电位, 以此为起点按 2 mV/s 的扫描速度对被测体系进行极化, 可测试出电极极化曲线。借助于塔费尔公式  $E-E_{\text{cor}}=a+blgi$ , 应用极化曲线外推法, 求出试样在不同温度、浓度中的腐蚀电流密度  $J_{\text{cor}}^{[6]}$ 。

## 2 结果与讨论

### 2.1 温度对各焊接接头腐蚀速率的影响

图 1a, b, c, d 为 7% 的亚硫酸铵溶液中不同温度下试样 1 号、2 号、3 号、4 号、5 号的极化曲线。从图可以看出, 各焊接接头在体系中发生了电化学腐蚀, 温度升高, 其自腐蚀电位逐渐降低。当温度在 20 ~ 80 °C 之间, 采用改性焊条焊接的接头极化率大于 J422 焊条焊接的接头和母材, 其中 Ni 元素含量为 1.2% 的接头极化率最大。从图 1d 还可以看出, 阳极极化曲线发生了钝化现象, 添加镍的接头致钝电流和维钝电流明显小于 J422 焊条的焊接接头和母材, 致钝电位明显高于普通 J422 焊条的焊接接头和

母材。这是由于镍的加入, 主要提高材料的电极电位而达到防腐目的<sup>[7]</sup>。表 1 是不同接头和母材在 20 ~ 80 °C, 7% 的亚硫酸铵介质中的自腐蚀电位和自腐蚀电流。由表 1 可知, 随着体系温度的升高, 各焊接接头自腐蚀电位逐渐降低, 腐蚀电流逐渐增大; 采用 J422 焊条焊接的接头自腐蚀电位低于母材, 而含镍的焊接接头的自腐蚀电位比普通 J422 焊条焊接的接头自腐蚀电位高, 自腐蚀电流小, 这说明焊缝含镍后自腐蚀电位得到提高, 从而使焊接接头在亚硫酸铵溶液中的耐蚀性得到提高。Ni 元素含量为 1.2% 的焊接接头的自腐蚀电位最高, 自腐蚀电流最小。这是因为当焊缝 Ni 元素含量为 1.2% 时, 焊缝组织晶粒细小致密, 提高了焊缝的腐蚀电位, 降低了焊接接头的腐蚀电流。

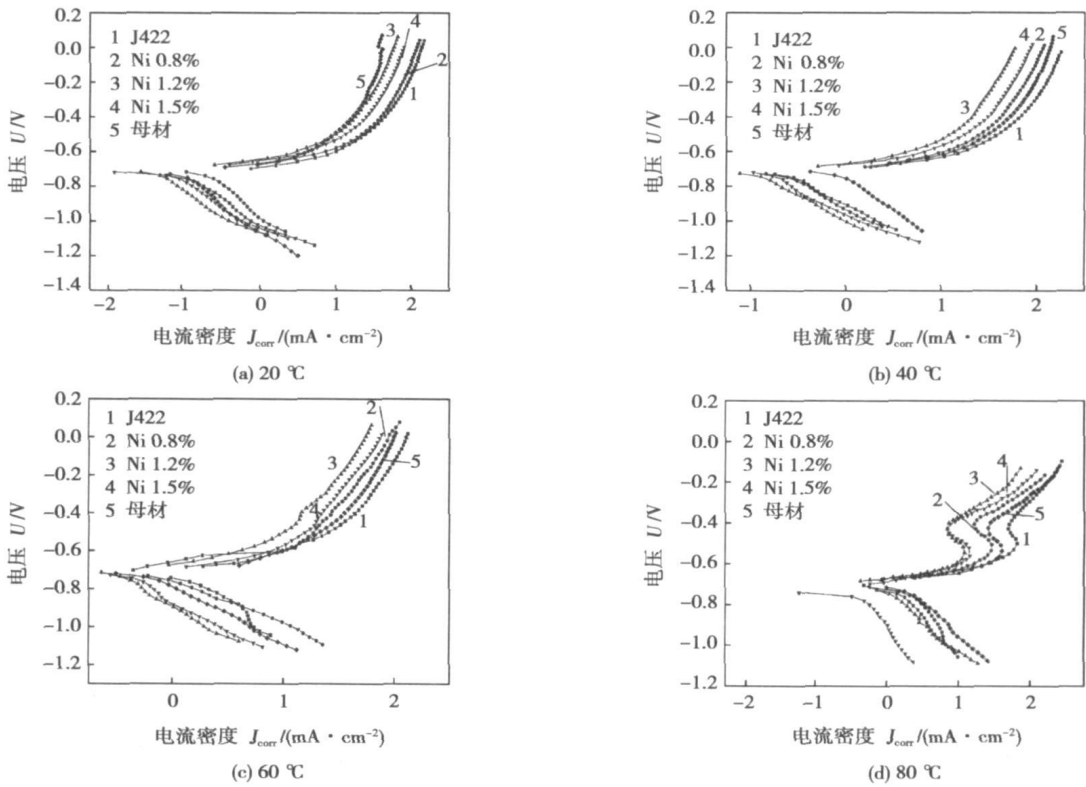


图 1 各焊接接头与母材在不同温度下、7% 的亚硫酸铵溶液中的极化曲线

Fig. 1 Polarization curves of different welded joint and base metal in 7% (NH<sub>4</sub>)<sub>2</sub>SO<sub>3</sub> at different temperature

### 2.2 浓度对各焊接接头腐蚀速率的影响

图 2a, b, c, d 为 40 °C 时不同浓度的亚硫酸铵溶液中试样 1 号、2 号、3 号、4 号、5 号的腐蚀极化曲线图。由图 2 可见, 随着亚硫酸铵浓度由 5% 增加至 11%, 极化曲线的形状均未发生明显变化, 仅是极化率发生了变化, 用改性 J422 焊条焊接的碳钢焊接接

头的极化率明显高于采用普通 J422 焊条焊接的接头和母材的极化率。表 2 为温度 40 °C, 各焊接接头在不同浓度的亚硫酸铵介质中的自腐蚀电位和自腐蚀电流。从表 2 中可以看出, 采用改性 J422 焊条焊接的接头在 5% ~ 11% 亚硫酸铵介质中, 自腐蚀电流比采用普通焊条 J422 所得的焊接接头的自腐蚀

表 1 7% 亚硫酸铵溶液中各焊接接头及母材的自腐蚀电位与自腐蚀电流

Table 1 Self-corrosion potential at corrosion current of welded joint in 7% (NH<sub>4</sub>)<sub>2</sub>SO<sub>3</sub> and different temperatures

试样编号	温度 $T/^\circ\text{C}$							
	20	40	60	80	20	40	60	80
	自腐蚀电位 $\varphi/V$				自腐蚀电流 $I/(10^{-5}\text{A})$			
1 号 J422	-0.698	-0.712	-0.719	-0.732	16.8	62.2	220	231
2 号 Ni 0.8%	-0.695	-0.700	-0.709	-0.718	9.1	51.4	145	206
3 号 Ni 1.2%	-0.688	-0.691	-0.697	-0.701	6.4	43.4	92.1	136
4 号 Ni 1.5%	-0.690	-0.694	-0.707	-0.714	9.0	50.1	97.7	161
5 号 母材	-0.697	-0.702	-0.714	-0.707	14.3	59.4	155	226

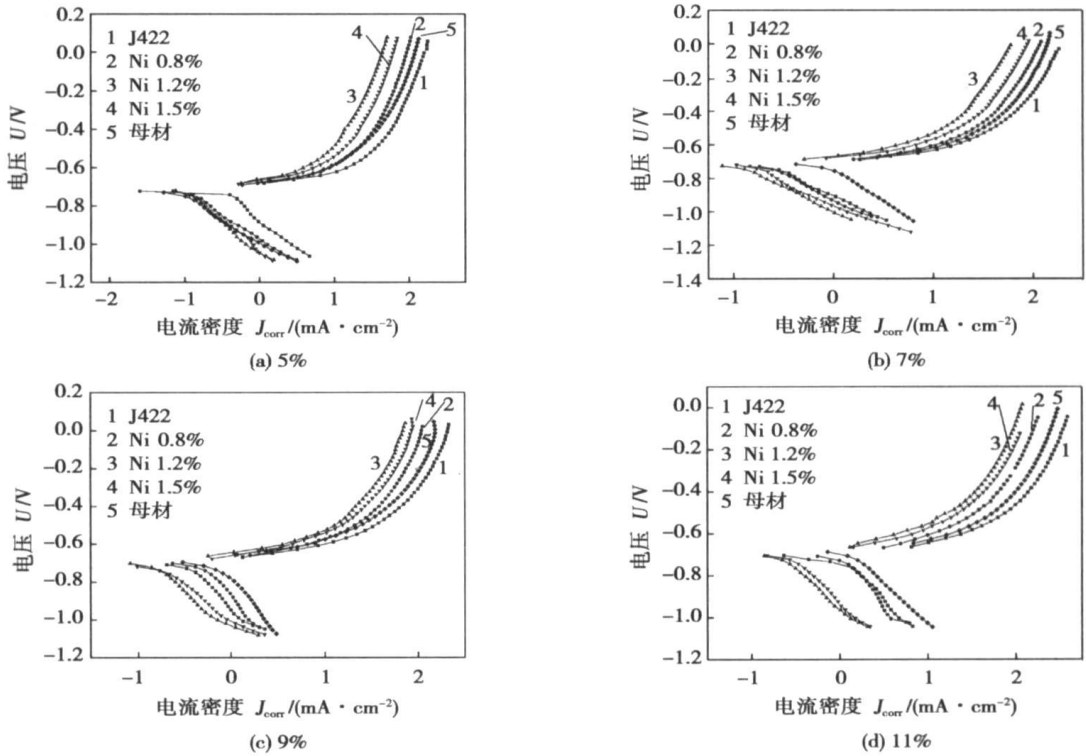


图 2 各焊接接头与母材在 40 °C 条件下、不同浓度的亚硫酸铵溶液中的极化曲线

Fig. 2 Polarization curves of different welded joint and base metal in (NH<sub>4</sub>)<sub>2</sub>SO<sub>3</sub> from 5%–11% at 40 °C

表 2 不同浓度亚硫酸铵溶液中各焊接接头及其母材的自腐蚀电位与自腐蚀电流

Table 2 Self-corrosion potential and corrosion current of welded joint in different concentration of (NH<sub>4</sub>)<sub>2</sub>SO<sub>3</sub> at 40 °C

试样编号	亚硫酸铵浓度 $w_{(\text{NH}_4)_2\text{SO}_3}(\%)$							
	5	7	9	11	5	7	9	11
	自腐蚀电位 $\varphi/V$				自腐蚀电流 $I/(10^{-5}\text{A})$			
1 号 J422	-0.711	-0.712	-0.715	-0.720	16.8	62.2	189	199
2 号 Ni 0.8%	-0.697	-0.700	-0.706	-0.709	9.1	51.4	76.5	141
3 号 Ni 1.2%	-0.689	-0.691	-0.693	-0.699	6.4	43.4	49.1	124
4 号 Ni 1.5%	-0.693	-0.694	-0.699	-0.702	9.0	50.1	72.3	137
5 号 母材	-0.699	-0.702	-0.710	-0.717	14.3	59.4	98.9	179

电流小。自腐蚀电流的大小次序是  $I_{J422} > I_{Q235} > I_{Ni0.8\%} > I_{Ni1.5\%} > I_{Ni1.2\%}$ 。由于腐蚀速率在电化腐蚀中与自腐蚀电流的大小相对应, 因此在 5% ~

11% 的亚硫酸铵介质中的腐蚀速率大小次序为  $v_{J422} > v_{Q235} > v_{Ni0.8\%} > v_{Ni1.5\%} > v_{Ni1.2\%}$ 。采用改性 J422 焊条的焊接接头中, 焊缝中由于镍的加入提高

了焊缝的自腐蚀电位,并相对于母材的自腐蚀电位高,使得焊缝相对于母材成阴极受到保护。Ni元素含量为1.2%的焊缝在5%~11%的亚硫酸铵介质中最耐蚀。由此可以认为,焊缝含镍量有最佳值,若含镍量较多,由于镍与铁的电位差较大,容易引起电偶腐蚀。因此适量镍的加入,可以有效地降低焊缝的腐蚀。

### 2.3 金相组织分析

图3为各焊缝的显微组织。图3a是普通焊条制备的焊缝的显微组织,由图3a可见焊缝组织中存在粗大的针状铁素体、魏氏体组织和少量夹渣。这种魏氏体组织的特点是粗大针状铁素体间具有伪珠光体组分,降低了焊接接头的耐蚀性。图3b, c, d为添加镍的焊缝显微组织,由图可见,随着焊缝镍含量增加,针状铁素体逐渐细化、减少,其中图3c即Ni元素含量为1.2%的焊缝晶粒细化且最均匀。这是Ni元素含量为1.2%的焊接接头耐蚀性较好的主要原因。分析进一步说明,焊缝Ni元素含量为1.2%的焊接接头具有良好的耐蚀性,而添加了镍元素的焊接接头又比J422焊条的焊接接头耐蚀。

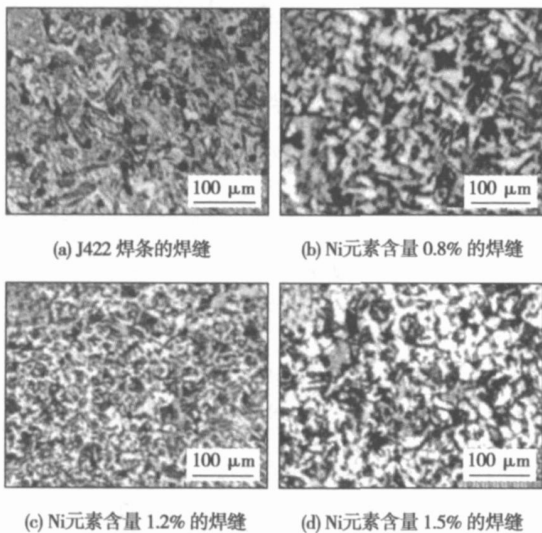


图 3 各焊缝的显微组织

Fig. 3 Microstructure of weld

## 3 结 论

(1) 用 J422 焊条焊接的焊缝组织中存在铁素体魏氏组织,这种魏氏组织的特点是粗大针状铁素体间具有伪珠光体组分,使焊接接头耐蚀性大大降低。用改性的 J422 焊条焊接后, Ni 元素含量为 1.2% 的焊缝晶粒细小、均匀,使焊接接头耐蚀性增强。

(2) 在亚硫酸铵溶液中,添加镍的改性焊条焊接的接头极化率较大,自腐蚀电位高于母材和 J422 焊条焊接的接头,而自腐蚀电流小于母材和 J422 焊条焊接的接头;即添加镍的焊接接头在亚硫酸铵介质中腐蚀速率小于母材和 J422 焊条焊接的接头。

(3) 焊缝含镍量有最佳值,若含镍量较多,由于镍与铁的电位差较大,容易引起电偶腐蚀。改性焊条焊接的焊缝 Ni 元素含量为 1.2% 时,接头在亚硫酸铵溶液中腐蚀速率最低。

### 参考文献:

- [1] 屈维均. 造纸工业化学分析[M]. 北京: 中国轻工业出版社, 1992.
- [2] 冯拉俊, 郭巧琴, 雷阿利. 碳钢焊接接头在亚硫酸铵溶液中的耐蚀性研究[J]. 中国造纸, 2006, 25(3): 25-28.
- [3] 顾 昀, 吴各风. 浅谈焊接与腐蚀[J]. 全面腐蚀与控制, 1999, 13(3): 32-34.
- [4] 上田修三. 结构钢的焊接—低合金钢的性能及冶金学[M]. 荆洪阳, 译. 北京: 冶金工业出版社, 2004.
- [5] 王 勇, 辛雁冰. 焊接接头腐蚀及微区测定[J]. 山东机械, 2000(1): 12-15.
- [6] 赵麦群, 雷阿利. 金属的腐蚀与防护[M]. 北京: 国防工业出版社, 2002.
- [7] 于福州. 金属材料的耐蚀性[M]. 北京: 科学出版社, 1982.

作者简介: 雷阿利, 女, 1957 年出生, 副教授。主要研究方向为金属的腐蚀与防护和材料加工。发表论文 30 余篇。

Email: leiali@126.com

Nanjing University of Technology, Nanjing 210009, China; 2. School of Mechanical and Power Engineering, East China University of Science and Technology, Shanghai 200237, China). p17–20

**Abstract** The residual stress generated in brazed process and its creep relaxation behavior for stainless steel plate-fin structure at high temperature were analyzed by finite element code ABAQUS. The results show that larger residual stress was generated in brazed joint due to the mismatch mechanical properties between brazing filler metal and base metal and the constraint of clamping fixture. At high temperature region, the residual stress was greatly decreased due to the creep relaxation behavior. The creep stress and strain are concentrated in the fillet zone, where the crack may initiate and propagate along the brazing seam.

**Key words:** stainless steel plate-fin structure; brazing residual stress; creep relaxation; finite element analysis

**Microstructure and wear resistance of laser cladding Co+Ni/WC alloy composite coating** YAN Yonggen<sup>1</sup>, SI Songhua<sup>2</sup>, ZHANG Hui<sup>2</sup>, HE Yizhu<sup>2</sup> (1. Baoshan Iron & Steel Co., Ltd. Shanghai 201900, China; 2. School of Material Science and Engineering, Anhui University of Technology, Maanshan 243002, Anhui, China). p21–24

**Abstract:** Laser cladding Co-based composite coating (Co+Ni/WC) have been obtained on low carbon steel substrate. Microstructure and wear resistance of the composite coatings were investigated compared with the Co-based coating (Co60). It is indicated that the Co60 coating was composed of primary dendrite of  $\gamma$ -Co and the eutectics of  $\gamma$ -Co+Cr<sub>23</sub>C<sub>6</sub> among the interdendrites, and Co+Ni/WC composite coatings were composed of  $\gamma$ -Co dendrite and the small eutectics which consists of  $\gamma$ -Co, Cr<sub>7</sub>C<sub>3</sub>, Co<sub>3</sub>W<sub>3</sub>C and unmelted WC particles. With more WC particles, there was further influence to Co60 coating that the directional solidification of dendrite was changed and the dendrite was finer. Owing to the Ni alloy wrapper, the WC particles had been protected from melt for the diffusion reaction on interface between the WC particles and the Co based alloy. Compared with Co60 coating, the hardness and wear resistance of the Co+Ni/WC composite coatings had been improved and the wear resistance of the Co+20%WC composite coating was twice of that of the Co60 coating.

**Key words:** laser cladding; Co-based alloy; microstructure; wear resistance

**An imaging model for X-ray system and its calibration method** TIAN Yuan<sup>1</sup>, DU Dong<sup>1</sup>, HOU Runshi<sup>1</sup>, GAO Zhiling<sup>2</sup>, SHEN Liqun<sup>2</sup> (1. Department of Mechanical Engineering, Tsinghua University, Beijing 100084, China; 2. Petroleum Steel Pipe Co., Ltd, Qingxian 062650, Hebei, China). p25–28

**Abstract:** It's one of the most extensive methods to inspect workpiece with X-ray and automatic inspection based on image processing is an important field. The imaging model and calibration establish a geometrical relationship between workpiece and its image, which is the precondition for automatic orientation and measurement with images. Ignored some factors such as the shape of the image in-

tensifier's input screen, the paper develops a model and calibration method for the imaging system used in automatic nondestructive testing system, which is used in weld defect inspection. The results show that the method is effective.

**Key words:** inspection with X-ray; weld defect; imaging model; calibration

**Corrosion of carbon steel joint used modified J422 electrode in ammonium sulfite** LEI Ali, ZHANG Shengchao, ZHANG Min (School of Materials Science and Engineering, Xi'an University of Technology, Xi'an 710048, China). p29–32

**Abstract** Since the welded joint of carbon steel is corroded seriously in the ammonium sulfite, corrosion behavior of welded joint welded by arc welding with J422 electrode containing different contents of Ni has been studied by means of three electrode galvanostatic test and metallurgical structure analyses. The results show that the addition of Ni causes the grain refinement of the weld and the decrease of acicular ferrite. In addition, the polarizability of the weld increases and the corrosion current decreases in the ammonium sulfite. The welded joint containing 1.2 wt% Ni has the lowest corrosion rate.

**Key words:** ammonium sulfite; weld decay; alloying; galvanostatic

**Displacement signal time-frequency domain analysis and quality judgment of aluminum alloy resistance spot welding** PAN Cunhai<sup>1</sup>, DU Sumei<sup>1</sup>, SONG Yonglun<sup>2</sup> (1. School of Mechanical Engineering, Tianjin University of Science and Technology, Tianjin 300222, China; 2. School of Electromechanical Engineering, Beijing University of Technology, Beijing 100085, China). p33–36

**Abstract** Resistance spot welding quality real-time monitoring of aluminum alloy was realized by distributed multiple-sensor synchronous collection system. Displacement signal time-frequency domain analysis shows that Butterworth band-pass filter range of the expulsion welding spot electrode displacement signal can reach about 0.5 mm between 40–80 Hz. The electrode displacement signal range of the undersize welding spots is lower about 1.0 mm than other two kinds of welding spots, so that using the explicit characteristic information can implement at resistance spot welding quality judgment by man and further can finish quality judgment by machine using the high signal-to-noise displacement signal and the brevity characteristic extracting method. At the same time, statistic analysis of 197 samples indicates that the percentage of accuracy can reach 97.6% at the acceptable welding spots zone.

**Key words:** resistance spot welding; aluminum alloy; displacement signal; time-frequency domain analysis; quality judgment

**Numerical simulation on flow and heat transfer in weld pool of laser-plasma hybrid welding** LI Zhining, DU Dong, CHANG Baohua, WANG Li (Key Laboratory for Advanced Materials Processing Technology, Ministry of Education, Tsinghua University, Beijing 100084, China). p37–40

**Abstract** A unified model is established for the liquid zone,